Dynamic optimisation of an industrial web process

Majeed Soufian*
Numerical Algorithm Group, Oxford, OX2 8DR, UK & Kellogg College,
Oxford University, Oxford, OX2 6PN, UK.
E-mail: majeed.soufian@nag.co.uk

ABSTRACT

An industrial web process has been studied and it is shown that the underlying physics of such processes governs by the Navier-Stokes partial differential equations with moving boundary conditions, which in turn have to be determined by the solution of the thermodynamics equations. The development of a two-dimensional continuous-discrete model structure based on this study is presented. Other models are constructed based on this model for better identification and optimisation purposes. The parameters of the proposed models are then estimated using real data obtained from the identification experiments with the process plant. Various simulation tests for validation are accompanied with the design, development and real-time industrial implementation of an optimal controller for dynamic optimisation of this web process. It is shown that in comparison with the traditional controller, the new controller resulted in a better performance, an improvement in film quality and saving in raw materials. This demonstrates the efficiency and validation of the developed models.

1. INTRODUCTION

Manufacturing of continuous webs of material is an important and growing technology, which can be found in many different industrial sites such as metal rolling mills, plastic and paper manufacturing. These processes are distributed parameters systems where the quality variables of the product such as thickness and basis weight vary in two dimensions, time (machine travel) and space (cross machine) [1,2].

This paper is concerned with the model development, multiphysics simulation and control of a plastic film extrusion process. It is important for quality control reasons that the film is manufactured with a uniform thickness, particularly across the web. Poor film thickness control results in excessive material wastage and leads to film winding difficulties later in the process. Further, a tighter thickness regulation makes it possible to obtain closer result to the target thickness and facilitate significant savings in raw material. Traditional industrial practice is to use multiple, single-input, single-output PI or PID controllers. There are also a number of publications based only on simulation studies, which examine the application of modern web process control such as Linear Quadratic (LQ) control [3-6]. The design, development and real-time industrial implementation of an optimal LQ controller for a plastic film extrusion process are presented here. This particular application produces a 2m wide film with a thickness ranging from 18 to 90 micron. Film thickness is measured using an infrared scanning gauge and exhibits significant transport delay. The control is achieved with 71 actuators distributed across the extruder die and is implemented using a low cost Programmable Logic Controller (PLC). The machine production rate is approximately 50 tons per month.

* Formerly Department of Engineering, Manchester Metropolitan University, Manchester. M1-5GD, UK.

In following, firstly the development of a two-dimensional continuous-discrete model structure based on fluid and thermo-dynamics considerations of the extrusion process for a laminar, isothermal, non-Newtonian and incompressible fluid using the Navier-Stokes partial differential equations is considered. Then the parameters of the proposed model have been identified using real data obtained from process plant. Moreover, based on this model a real-time controller is designed and implemented on an industrial platform. In comparison with the traditional controller, the new controller presented an improved performance. This demonstrates the efficiency and validation of the developed model.

2. MODELLING OF THE PROCESS PLANT

The process of film making from a modelling point of view includes extrusion, actuators, stentering and a measurement phase (Figure 1). In the following sections, each phase is studied in some details and equations governing them are studied for model structure selection and simulation purposes.

2.1. THE UNDERLYING PHYSICAL BEHAVIOUR OF THE PROCESS

One of the most important quality variables of the product is the thickness. Film thickness depends on many factors including die gap, extrusion pressure, temperature and flow rate as well as cooling rate and film tension [7, 8].

2.1.1. Dynamics of fluid parts

Continuous plastic film is produced by extrusion of a plasticized polymer material through a narrow slit shaped die. In order to obtain the dynamical behaviour of this part, a three-dimensional analysis of the moving fluid inside the extrusion die is required. This can be achieved by solving a system of five simultaneous partial differential equations, which are: mass conservation equation, the *x*-, *y*- and *z*- components of momentum equation and energy equation known as the Navier-Stokes equations [9,10]. Consider the extrusion die shown in Figure 2. The molten polymer is forced at a steady rate from a large reservoir into an extruder lip of length l and small width D. We shall assume, an isothermal flow of an incompressible fluid and a length of lip much greater than its diameter: i.e. $l/D>>1$. The co-ordinate system is defined in Figures 1 and 2. It can also be assumed that the entrance and exit losses are negligible. The continuity equation can then be written as:

$$\frac{\partial \rho}{\partial t}+\frac{\partial}{\partial x}(\rho V_x)+\frac{\partial}{\partial y}(\rho V_y)+\frac{\partial}{\partial z}(\rho V_z)=0 \tag{1}$$

In this case density ρ is assumed to be constant if the temperature θ of molten plastic is kept constant. The *x*-, *y*- and *z*- component of momentum equation can be written as:

$$\rho\frac{D}{Dt}V_x=-\frac{\partial P}{\partial x}+\frac{\partial \tau_{xx}}{\partial x}+\frac{\partial \tau_{yx}}{\partial y}+\frac{\partial \tau_{zx}}{\partial z}+S_{Mx} \tag{2}$$

$$\rho\frac{D}{Dt}V_y=-\frac{\partial P}{\partial y}+\frac{\partial \tau_{xy}}{\partial x}+\frac{\partial \tau_{yy}}{\partial y}+\frac{\partial \tau_{zy}}{\partial z}+S_{My} \tag{3}$$

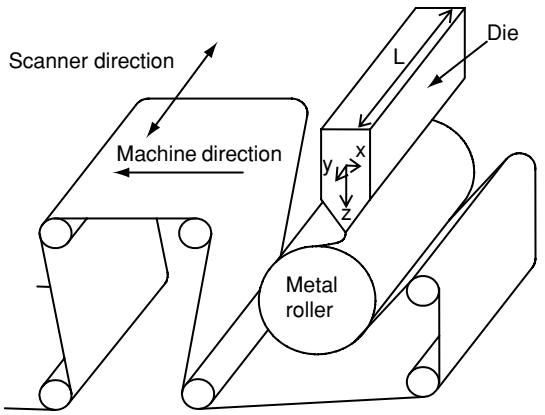

Figure 1 A simplified schematic of the film extrusion process.

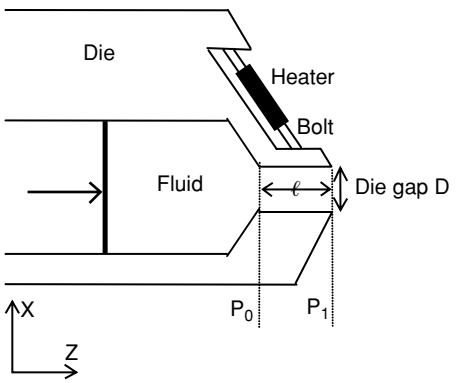

Figure 2 A simplified schematic of the extrusion die.

$$\rho \frac{D}{Dt} V_z = -\frac{\partial P}{\partial z} + \frac{\partial \tau_{xz}}{\partial x} + \frac{\partial \tau_{yz}}{\partial y} + \frac{\partial \tau_{zz}}{\partial z} + S_{Mz} \tag{4}$$

where the first operator in above equations is the total or substantive derivative which is defined as:

$$\frac{D}{Dt} \equiv \left(\frac{\partial}{\partial t} + V_x \frac{\partial}{\partial x} + V_y \frac{\partial}{\partial y} + V_z \frac{\partial}{\partial z} \right)$$

In the normal operation conditions, molten polymer is forced at a steady rate in the direction of extrusion lip, i.e. ($\partial P/\partial t$=0), the fluid only moves in that direction within the lip. Also the boundary in direction y is assumed to be at physical infinity i.e., L/D>>1, so the surface

effect of boundary at y can be ignored. Therefore $V_x = V_y = 0$, $V_z \neq 0$, and $V_z = f(x)$ only, for the developed profile since $L/D >> 1$. The source terms S_{Mx}, S_{My} and S_{Mz} are related to the contribution of body forces. Then only the contribution of gravity can be accounted here so $S_{Mx} = S_{My} = 0$ and $S_{Mz} = \rho g$. From the above constraints imposed on the system and above mathematical equations, the shear stress profile across the extruder lip for the fluid can be obtained as:

$$\tau_{xz} = \frac{\Delta P}{\ell}|x| \tag{5}$$

where $\Delta P = P_1 + \lambda \times S_{Mz} - P_0$ is a fixed value and assuming that shear stress at $x = 0$ is zero. In this application, the rheological properties of the fluid can be used without considering energy equation. The power law constitutive equation known as the Ostwald-de Waele model of molten plastic can be written as:

$$\tau_{xz} = -K|\dot{\gamma}|^{n-1}\dot{\gamma} \tag{6}$$

where K and n are assumed to be constants, $\dot{\gamma} = (dV_z/dx)$ and $|\,dV_z/dx\,| = -dV_z/dx$, thus

$$K\left|\frac{dV_z}{dx}\right|^n = \frac{\Delta P}{\ell}|x| \tag{7}$$

Considering no-slip at the wall, the boundary condition in x direction is: $V_z(x = \pm D/2) = 0$, where D is assumed to stay constant. Then the constitutive equation for the velocity profile of melton polymer in extruder lip can be derived as:

$$V_z(x) = \frac{n}{n+1}\left(\frac{\Delta P D^{n+1}}{2^{n+1} K \ell}\right)^{\frac{1}{n}}\left[1 - \left(2\frac{|x|}{D}\right)^{\frac{n+1}{n}}\right] \tag{8}$$

This implies that the volumetric flow rate of the fluid Q through the extruder lip can be calculated knowing the fluid velocity profile:

$$Q = \iint_S V dx dy$$

where S is the ending cross section area of the extruder lip. Then the output flow of a small element $\Delta y(y)$ in position y will be:

$$Q(\Delta y) = \frac{2n}{2n+1}\left(\frac{\Delta P}{K\ell}\right)^{\frac{1}{n}}\left(\frac{D}{2}\right)^{\frac{2n+1}{n}}\Delta y \tag{9}$$

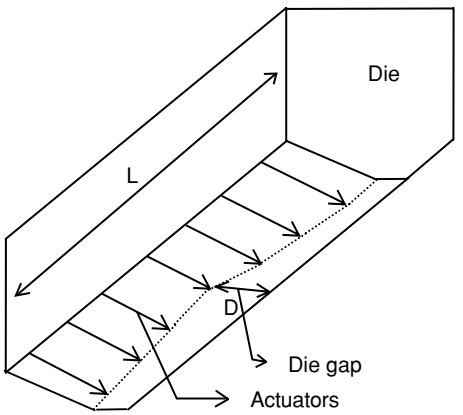

Figure 3 The actuators and moving boundaries.

It is evident that knowing the $Q(\Delta y)$ and the velocity of machine V_m , the thickness of web at any location can be predicted easily by:

$$\Delta x = \frac{Q(\Delta y)}{V_m \Delta y \Delta t} \tag{10}$$

As it is apparent from above equations, in steady state where D, ΔP and V_m are constants, the relationship between the qualitative variables shows a static map. Furthermore, the output flow rate and thickness of the film also stay constant.

2.1.2. Moving boundary conditions, dynamics of the actuators

Cross-directional variations of thickness are controlled by alteration of the die lip gap D. The gap D at each specific location across the web wide is adjusted by using the thermal expansion of die bolts which are spaced at regular intervals across the entire width of the die (Figure 3). Therefore, $D \in R^+$ is a function of y and is determined by the dynamics of the die bolt at that point and interaction with neighbourhood bolts, i.e.:

$$\frac{\partial D(y_i)}{\partial t} = -\frac{\alpha \ell_0}{mc}\left(W_{in}(y_i,t) - \frac{\partial Q_{loss}(y_i)}{\partial t} + \frac{\partial Q_{\text{int}r}(y_i)}{\partial t} \right) \qquad i = 1, 2, ..., n_y \tag{11}$$

The individual bolts are heated by electrical cartridges, which are controlled using pulse width modulation. This method of manipulating the die gap has the advantage of providing very small movements, in the order of a few microns, but has the disadvantage of exhibiting very slow dynamics. The terms $W_{in}(y_i, t)$, $Q_{loss}(y_i)$ and $Q_{intr}(y_i)$ are respectively input power to electrical heating cartridge located at $y_i = Li/n_y$ (or simply i-th one), the lost heat and heat observed from neighbourhood cartridges. The major heat loss will be by convection in the process plant. The heat transfer rate is determined by using Newton's law of cooling:

$$\frac{\partial Q_{loss}(i)}{\partial t} = hS_{loss}\left(\theta_{die,i} - \theta_{env}\right) \tag{12}$$

where S_{loss} is the surface area through which heat transfer takes place, the $\theta_{die,i}$ and θ_{env} are the temperature of i-th die bolt and environment, respectively. The heat transferred between the die bolts will be carried out by conduction and according to Fourier's law:

$$\frac{\partial Q_{\mathrm{int}r}(i)}{\partial t} = -k_t S_{con}\frac{\partial \theta_i}{\partial y} \tag{13}$$

where S_{con} is the area normal to the direction of heat transfer, and is inversely proportional to the thickness of the layer. The die bolts are spaced at regular intervals $\Delta L = L/n_y$ across the entire width of the die. It is obvious that integrating both side of Eqn 13 yields:

$$\frac{\partial Q_{\mathrm{int}r}(i)}{\partial t} = -n_y k_t S_{con}(2\theta_{die,i} - \theta_{die,i-1} - \theta_{die,i+1})/L \tag{14}$$

The behaviour of $D(y_i)$ can be obtained by solving Eqns 11, 12 and 14. Between each cartridge $D(y)$ can be approximated using a linear interpolation. The dynamics of boundaries can effect the basic assumptions made in the previous section i.e. $L/D>>1$, $l/D>>1$, $V_x = V_y = 0$, $V_z \neq 0$, $V_z \neq f(y)$ and $V_z = f(x)$ so that the simultaneous partial differential Eqns 1 to 4 and Ostwald-de Waele equation can no longer be solved analytically. However, as it appears from the physics of the problem and normal operation conditions of the process, the variation in D is very small and uniform. This satisfies above assumptions and Eqns 8 to10 are then valid even when D is a dynamical variable with a limited range of variations.

2.1.3. The stentering phase

The extruded material is chilled and solidified into a film on the surface of a metal roller. It is also stretched and drawn in a direction perpendicular to MD using a tentering frame. Tension in the film tends to cause it to shrink laterally. To reduce shrinkage, electrostatic discharge heads are used to charge the film at the edges causing it to be pulled laterally and stick to the roller.

Although the die bolts are evenly spaced across the film at the die lip, the stentering causes the effective location of the die bolt position to change and makes the estimation of the position of die bolt centres difficult (Figure 4). The experiences show that the relationship between actuators and their positions across the web in stentering phase can mathematically be modelled as a static map rather than a dynamic one. In practice there is a lookup table to describe this map.

2.1.4. The film thickness measurement and transport delay

On completion of this process, the film is cooled using cooling rolls and then scanned to measure film thickness before being stored on a reel. Variations in the film thickness are measured using an infrared scanning gauge, which moves back and forth across the width of the plastic (Figure 5). So scanning gauge measures simultaneously both the cross directional and the machine directional variations.

There is also a large transport delay that exists between the control actuators and the measurement device due to the distance from the die to the scanning gauge. The transport delay varies with machine speed but also with the position across the film since it takes a

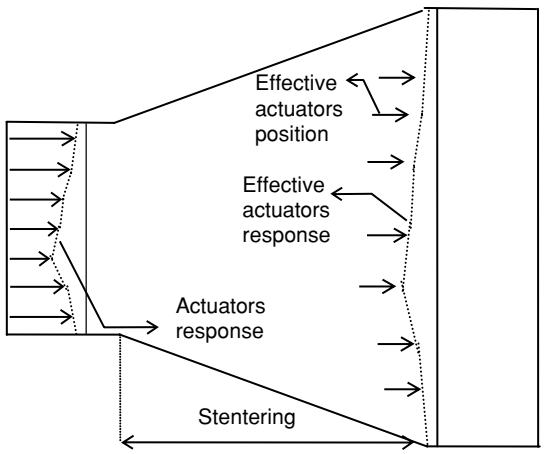

Figure 4 The overhead view of the effect of stentering phase.

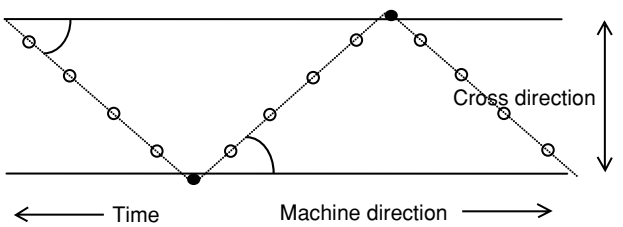

Figure 5 The overhead view of the cross directional scans using infrared gauge.

significant time for the measuring head to traverse across the film. Since the scanning head traverses the film in both directions, the delay period can vary for different scans.

2.1.5. Summary and conclusion

From a qualitative standpoint, the above analysis shows proper trends and can be useful for model structure selection and simulation. Actual flow data tends to be quantitatively different from analytical predictions even when a fixed boundary conditions is practised. The reason is that n is a function of dV_z/dx and dV_z/dy, so n tends to depend on Q. There is also no guarantee that temperature and the density distribution of molten polymer stay uniform and constant in whole of die extruder. On the other hand, from a rheological point of view, there is no substitute for experiments and therefore the dynamical parameters of the web process must be obtained experimentally using measured data.

2.2. EXPERIMENTAL MODELLING

The first step of any experimental modelling is essentially concerned with the problem of representation, i.e., to specify and parameterise a class of mathematical models to represent the system to be identified [11–14].

2.2.1. Model structure selection

The plastic extrusion process is a 2-D system, with variations occurring along the film length and across the film width. Several methods are used to represent the 2-D systems, for

example: transfer functions, partial difference equations, convolution summation, and state-space models. A transfer function model was used in [15] for the development of linear optics. A 2-D ARMA model was written in [16] as:

$$A(v^{-1},w^{-1})\, y(i,j) = B(v^{-1},w^{-1})\, u(i,j) + C(v^{-1},w^{-1})\, e(i,j) \tag{15}$$

where y is the output and e is zero mean white noise of variance σ_e^2. The i and j represent the co-ordinates in plane with respect to some arbitrary origin. The shift operators v^{-1} and w^{-1} represent operations in i and j co-ordinates respectively. For a Quarter-Plane (QP R(M,N)) region of support, the polynomials of A, B and C are given by:

$$A(v^{-1},w^{-1}) = \sum_{m=0}^{M_a}\sum_{n=0}^{N_a} a_{m,n}\, v^{-m}\, w^{-n}$$

$$B(v^{-1},w^{-1}) = \sum_{m=0}^{M_b}\sum_{n=0}^{N_b} b_{m,n}\, v^{-m}\, w^{-n}$$

$$C(v^{-1},w^{-1}) = \sum_{m=0}^{M_c}\sum_{n=0}^{N_c} c_{m,n}\, v^{-m}\, w^{-n}$$

The coefficients $a_{m,n}$, $b_{m,n}$ and $c_{m,n}$ are respectively associated with the auto-regressive, the inputs and the moving average parts of the model. The maximum of m and n determines the support area for each part.

Habibi [17] described a model for estimating images in presence of noise based on partial difference equations. Also a state space model was introduced in [18] for linear iterative circuits. In past three decades a special attention has been given to the definition and analysis of stationary 2-D state space models. All models are quarter plane causal. In 1972, Givone-Roesser [19] considered the first quadrant-causal systems as:

$$\begin{bmatrix} x^h(i+1,j) \\ x^v(i,j+1) \end{bmatrix} = \begin{bmatrix} A_1(i,j) & A_2(i,j) \\ A_3(i,j) & A_4(i,j) \end{bmatrix} \begin{bmatrix} x^h(i,j) \\ x^v(i,j) \end{bmatrix} + \begin{bmatrix} B_1(i,j) \\ B_2(i,j) \end{bmatrix} u(i,j)$$
$$y(i,j) = \begin{bmatrix} c_1(i,j) & c_2(i,j) \end{bmatrix} \begin{bmatrix} x^h(i,j) \\ x^v(i,j) \end{bmatrix} \tag{16}$$

where $x^h \in R^n$ and $x^v \in R^m$ represent the horizontal and vertical states respectively, u is the input and y is the output. Fornasini-Marchesini (F-M) have considered the 2-D state space model in some details [20]. The F-M model can be described as:

$$X(i+1, j+1) = A_1(i, j+1)\, X(i, j+1) + A_2(i+1, j)\, X(i+1, j) + A_0(i, j)\, X(i, j) + B(i, j)\, u(i, j) \tag{17}$$
$$y(i, j) = c(i, j)\, X(i, j)$$

where $X \in R^n$, $u \in R^p$ and $y \in R^q$. Because of the appearance of both $X(i+1, j+1)$ and $X(i, j)$

terms, it is clear that the above equation is not a first order difference equation. In a series of studies, Porter-Aravena [21] have purposed a modified version of F-M which is called Modified F-M model. It uses the following state model for presenting a given 2-D system:

$$\begin{aligned} X(i+1, j+1) &= J(i, j+1)\,X(i, j+1) + K(i+1, j)\,X(i+1, j) + E(i, j+1)\,u(i, j+1) + F(i+1, j)\,u(i+1, j) \\ y(i, j) &= c(i, j)\,X(i,j) \end{aligned} \quad (18)$$

where matrices $\boldsymbol{J}(i, j+1)$, $\boldsymbol{K}(i+1, j)$, $\boldsymbol{E}(i, j+1)$ and $\boldsymbol{F}(i+1, j)$ are of appropriate dimensions. This model has the advantage of being first order difference equations.

The model Eqns 15 to 18 are generic 2-D models and it is not clear that their structure are appropriate for processes such as plastic extrusion. The physical modelling of the target process can help to derive an appropriate model or model structure in the form of partial/ordinary differential or difference equations. Using the analysis presented in previous sections and Eqns 8 to 14, a model structure for the target process is suggested in the following form:

$$\frac{dx(i,t)}{dt} = r_{i-1}x(i-1,t) - f_i\,x(i,t) + r_{i+1}\,x(i+1,t) + g_i\,u(i,t-d) + \varepsilon(i,t) \quad (19)$$

where $r_i \in R^+, f_i \in R^+ g_i \in R^+$ and time delay $d \in R^+$ are the coefficients or parameters of the model, and u, x and ε are input power, measured thickness and zero mean white noise of variance σ_e^2 respectively. This model structure of the process plant is described by a 2-D discrete-continuous equation where the state variable $x(i,t)$ depend on two independent and indeterminate variable $i \in Z^+$ and $t \in R^+$.

2.2.2. Identification experiment and model parameter estimation

After obtaining a model structure based on the underlying physical behaviour of the process, the coefficients of the model have to be determined using parameter identification techniques [11]. Please note that the identifiability of 2D discrete-continuous models for nontrivial processes is not a trivial issue and has not been fully investigated yet. This is especially important for achieving accurate parameter estimation resulting from an unbiased estimation procedure [12, 13]. Considering this fact and using a specific scanning regime for film thickness measurement it is possible to rewrite the suggested model Eqn 19 as a square state space model, i.e.:

$$\frac{dX(t)}{dt} = \mathbf{F}X(t) + \mathbf{G}U(t-d) \quad (20)$$

$$Y(t) = \boldsymbol{C}\,X(t) + E(t)$$

where $X(t)$, $Y(t)$, $U(t)$ and $E(t)$ are augmented vector of state variables, output, input and white noise respectively. Here it is assumed that the number of inputs, which is the number of heated die bolts, is qual to the number of outputs, which is the number of samples captured by the thickness gauge as it scans the film. Then matrices **F**, **G** and **C** are square and have appropriate dimensions with specific structures:

$$\mathbf{F}=\begin{bmatrix} -f_1 & r_2 & \cdots & \cdots & 0 \\ r_1 & -f_2 & r_3 & & \vdots \\ \vdots & r_2 & -f_3 & \ddots & \vdots \\ \vdots & & \ddots & \ddots & r_{n_y} \\ 0 & \cdots & \cdots & r_{n_y-1} & -f_{n_y} \end{bmatrix}, \quad \mathbf{G}=\begin{bmatrix} g_1 & 0 & \cdots & 0 \\ 0 & g_2 & & \vdots \\ \vdots & & \ddots & \vdots \\ 0 & \cdots & \cdots & g_{n_y} \end{bmatrix} \tag{21}$$

and **C** is a unity matrix. More important the matrix **F** is a Metzler matrix [22], which is a stability matrix and shows the system under consideration is stable. In order to obtain estimates of the model parameters, a series of open-loop experiments were performed. To run the identification experiments, a form of test signal is needed for the system inputs. Theoretically the best choice for a test signal is an optimal input signal, which minimises certain model errors with respect to noise, input and output signal constraints and measuring time. It assumes the use of an asymptotically efficient parameter estimation so that the parameter covariance matrix can be approximated. However, because of practical difficulties only open-loop step response tests were carried out on the die bolts, individually and in-groups [23]. The resulting scanned thickness measurements were captured by a PC for analysis and parameter estimation. There are many unbiased estimation procedure available mostly based on least square methods, which produce an accurate estimation of the parameters [24, 25]. The proposed model structure was found to fit the measurements well. The parameters were estimated as follows:
$f_1 = f_{ny} = 0.0053$, $f_i = 0.0087\ \forall\ i =]1, n_y[$, where $n_y = 71$, $r_i = 0.0034$, $g_i = 0.0019 \forall\ i \in [1, n_y]$ and d = 114 seconds, which can be substituted in the desired Eqns 19 or 20 and 21 to yield the relevant model.

2.2.3. Simulation and accuracy of the obtained model in practice

Apart from analysing estimation procedure and its results to ensure having unbiased estimation, a series of practical tests were conducted to see how well simulation based on obtained model will follow real response of the process plant for both normal operation condition and irregular operation of the plant. It was noted that when a large number of adjacent bolts were stepped by a large amount there were dynamic effects, which were not predicted by the model. Figures 6 and 7 show a part of a typical open-loop step response test of the model and process plant respectively, as power to the die bolts 20 to 40 was suddenly changed by 40% reducing the material thickness. The material adjacent to the stepped bolts shows some thickening even though these die bolts were held constant. This effect is due to the non-uniform and large movement of boundary in *x* direction. Thus the basic assumptions made in section 2 is no longer valid and $V_x \neq 0$, $V_y \neq 0$, $V_z \neq 0$, $V_z = f(x, y)$ and polymer bulk will move laterally within the die. The Navier-Stokes equations no longer can be solved analytically and rigorous numerical method of Computational Fluid Dynamics (CFD) is required to produce a numerical approximation. The proposed model based on analytical solution of Navier-Stokes equations does however give good results when the die bolt perturbations are relatively small and locally non-uniform or they are large but globally uniform. Figures 8 and 9 investigate this and show the velocity profiles for a uniform change and a small non-uniform movement of boundaries in x direction, respectively. Since this is the normal case, under closed-loop regulation, it was decided that the model should suffice for standard operations of the process plant.

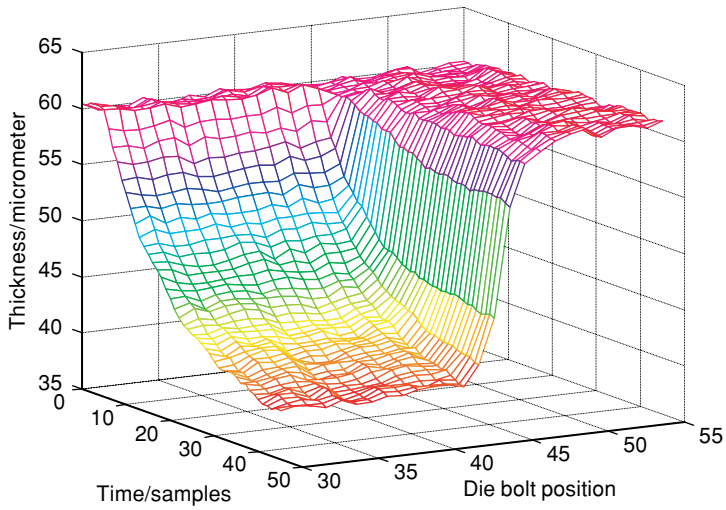

Figure 6 The prediction of model for a large input.

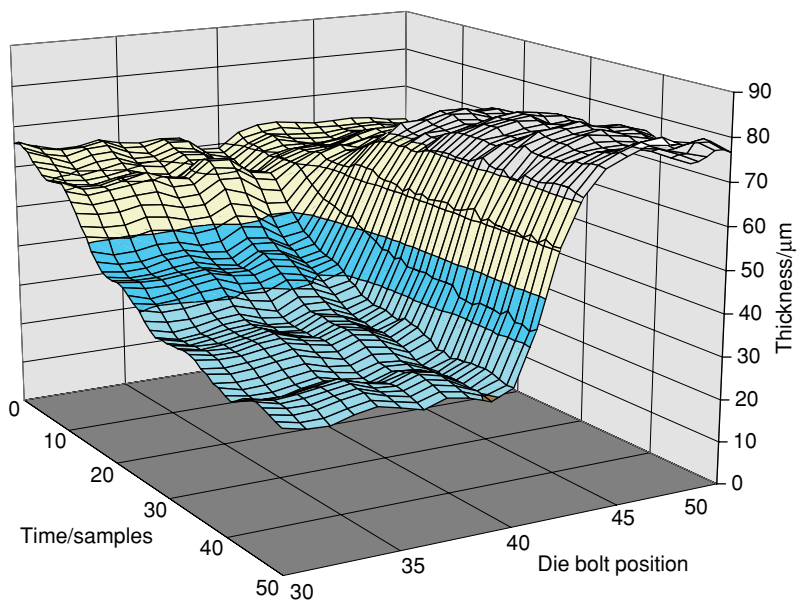

Figure 7 The response of system to the same large input.

3. CONTROL DESIGN

Film thickness control is concerned with variations occurring both along the film length and across the film width. Bulk film thickness is affected by regulation of the extrusion screw speed, extrusion speed, flow condition, uniform distribution of melt temperature and lip gap. Assuming that these quantities are kept within satisfactory tolerance, the cross-directional variations of the thickness are determined by alteration of the die lip gap. Given a linear

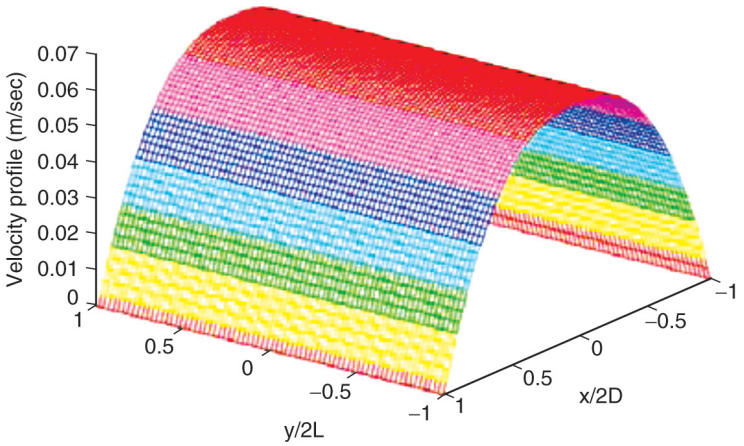

Figure 8 The velocity profile did not change its shape for a uniform movement of boundaries in x direction.

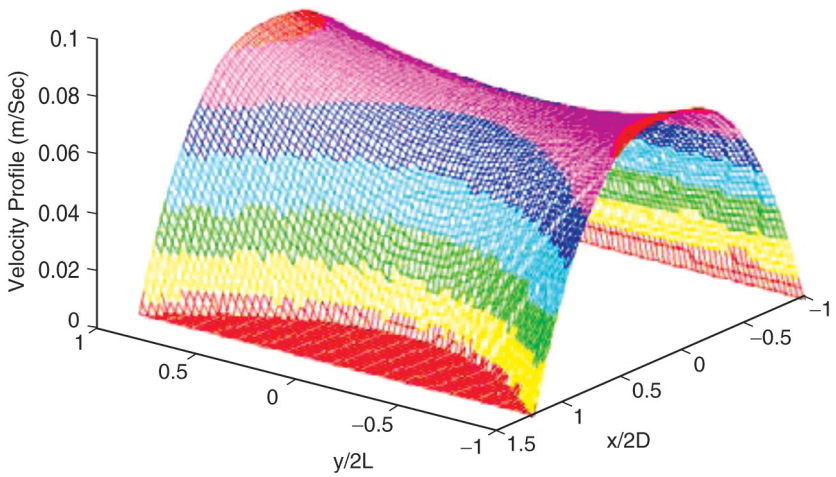

Figure 9 The change of velocity profile for a maximum of %10 increase in lip gap boundaries in x direction.

model of the process plant, it is desirable to design and synthesise a control scheme to control the multicomponent vector of state variables X through the use of the multicomponent vector of manipulated variable U and adjust the lip gap across the entire width of the die, therefore to achieve uniform thickness across the width of the film, to compensate for transport delay and allows a tighter regulation.

3.1. OPTIMAL CONTROL DEVELOPMENT

The control development is split into three parts: an optimal controller based on the delay free model, a predictor to overcome the effects of the transport delay and an integrator to summate the incremental control effort. The controller output is applied to the die bolts at

each sampling period T, via a zero-order hold. Ignoring any transport delay for the moment, the continuous-discrete time model of the process plant can be converted to a full discrete form:

$$x(i,k+1) = \sum_{j=-N}^{N} a_{i-j} x\left(i-j,k\right) + \sum_{j=-M}^{M} b_{i-j} u\left(i-j,k\right) \tag{22}$$

where $M \in Z^+$, $N \in Z^+$, $i\text{-}j > 0$, k is sampling interval, i.e. $t = k\,T$, and coefficients a and b decay when j increases. In terms of multicomponent vector of state variables $X(k)$:

$$X(k+1) = \mathbf{A}X(k) + \mathbf{B}U(k) \tag{23}$$

where $\mathbf{A} = (\mathbf{I}\text{-}T\mathbf{F})^{-1}$, $\mathbf{B} = (\mathbf{A} - \mathbf{I})\mathbf{F}^{-1}\,\mathbf{G}$ and T is sampling time. In order to ensure steady-state reference tracking with no offset, the control law is synthesised to calculate the incremental control effort $\Delta U(k) = U(k)–U(k–1)$ so automatically incorporating integral action. The plant model is therefore expressed in terms of $\Delta U(k)$:

$$\Psi(k+1) = \alpha\,\Psi(k) + \beta\Delta U(k) \tag{24}$$

where $\Psi \in R^{2n}$, $\alpha \in R^{2n \times 2n}$, $\beta \in R^{2n \times n}$, $\Delta U \in R^{n}$, and

$$\Psi(k+1) = \begin{bmatrix} X(k+1) \\ X(k) \end{bmatrix}, \quad \boldsymbol{\alpha} = \begin{bmatrix} \mathbf{A}+\mathbf{I} & -\mathbf{A} \\ \mathbf{I} & \mathbf{0} \end{bmatrix}, \quad \beta = \begin{bmatrix} \mathbf{B} \\ \mathbf{0} \end{bmatrix}$$

Given the linear model Eqn 24, the LQ controller is designed to minimise the quadratic cost criterion with symmetric and positive semi-definite matrices **Q** and **P**:

$$\underset{\Delta U(k),\ldots,\Delta U(k+N)}{Min} \left\{ \underset{N\to\infty}{Lim} \sum_{j=1}^{N} \left[e(k+j)^{\sim}\mathbf{Q}\,e(\mathbf{k}+\mathbf{j}) + \Delta U^{\sim}(k+j-1)\;\mathbf{P}\;\Delta U(k+j-1) \right] \right\} \tag{25}$$

where e is the error vector (r-Ψ), and r is the desired thickness or set point. N is the horizon for minimisation and is chosen large enough so that the control prediction extends to the steady state and the cost function converges. In such circumstances a fixed gain controller arises which may be considered to be acting on a projected horizon to infinity. The minimisation analysis can utilise a normalised model, which has the advantage of simplifying the initial selection of weights for **P** and **Q**. The controller that results from the minimisation of the cost function is given by:

$$\Delta U(k) = \mathbf{K}\,e(\mathrm{k}) \tag{26}$$

where $K = -\,(\beta^{\sim}\boldsymbol{R}\beta + \boldsymbol{P})^{-1}\,\beta^{\sim}\,\boldsymbol{R}\,\alpha$ and $\boldsymbol{R}$ is the steady-state solution of the Riccati equation:

$$\mathbf{R}(k) = \boldsymbol{\alpha}^{\sim}\mathbf{R}(k+1)\boldsymbol{\alpha} - \boldsymbol{\alpha}^{\sim}\mathbf{R}(k+1)\boldsymbol{\beta}\left(\boldsymbol{\beta}^{\sim}\mathbf{R}(k+1)\boldsymbol{\beta} + \mathbf{P}\right)^{-1}\;\boldsymbol{\beta}^{\sim}\boldsymbol{\rho}(k+1)\boldsymbol{\alpha} + \mathbf{Q} \tag{27}$$

The direct backward solution of above equation is possible but it is slow and not very accurate. Several algorithms are available for obtaining a solution to Eqn 27 such as Schur Vector Method, Generalised Schur Method and eigen-decomposition or spectral factorisation

[24,25]. Schur decomposition methods perform well even for repeated eigenvalues, however here eigenvector decomposition has been considered adequate and was used for solving above equation and calculating steady-state feedback gain matrix **K**. Then the control law can be synthesised to determine the incremental control effort at each sample *k*.

3.2. CONTROL REALISATION

It is assumed that all states are directly available for measurement and there is no need for state estimation. This is true assumption as **C** and *E* in Eqn 20 are represented respectively with a unity matrix and a vector whose elements are zero mean white noise of variance σ_e^2. The LQ controller developed above assumes a delay free plant, i.e. the feedback of thickness information is available immediately. With the transport delay, the plant model Eqn 24 can be written as:

$$\Psi(k + d + 1) = \alpha\, \Psi(k + d) + \beta\Delta U(k) \tag{28}$$

where *d* is the transport delay in samples. The direct application of the LQ controller (Eqn 26) to a system with transport delay results in an unrealisable controller. Ignoring transport delay causes instability in any closed-loop system. The control is unrealisable since it requires calculation of the control effort $U(k)$ based on future measurements, $\Psi(k+d)$, which are not available at current sampling time *k*, i.e.:

$$\Delta U(k) = \mathbf{K}\, e(k+d) = \mathbf{K}[r - \Psi(k + d)] \tag{29}$$

considering constant setpoint *r*. To rectify this, the predicted state of the plant at time k + d can be obtained from current state by substituting each future state Ψ(k + i) in the control law by its previous state Ψ(k + i-1) and control using process model to current state, i.e.:

$$\begin{aligned}\hat{\Psi}(k + d) &= \alpha^d\, \Psi(k) + \alpha^{d-1}\, \beta\Delta U(k - d) + \alpha^{d-2}\, \beta\Delta U(k - d+1) + \ldots \\ &+ \alpha^{d-i}\, \beta\Delta U(k - d+i - 1) + \ldots + \beta\Delta U(k - 1)\end{aligned} \tag{30}$$

where in above eqution $i \in Z^+$ and $i \in [1,d]$. This can be written in a compact form:

$$\hat{\Psi}(k+d) = \alpha^d \Psi(k) + \sum_{i=1}^{d} \alpha^{d-i} \beta\Delta U(k - d + i - 1)$$

Now the state at time k+d can be replaced by its prediction, resulting in the controller:

$$\Delta U(k) = \mathbf{K}\left[r - \alpha^d \Psi(k) + \sum_{i=1}^{d} \alpha^{d-i}\ \beta\Delta U(k - d + i - 1) \right] \tag{31}$$

The above multicomponent control vector is now realisable giving optimal performance with zero offset and the ability to deal with time delay. The closed-loop form can be obtained by substitution of Eqn 31 into the Eqn 28. This yields a recursive difference equation in terms of $\Delta U(k)$, which can be solved numerically. However the responses of the closed-loop system were simulated using a simulated environment [26] and are shown in Figures 10 and 11. These simulations presented a stable response as expected with a great performance compare to real closed-loop response of the current process plant. Although these are encouraging results and prove the principles, there are many practical issues such as safety, un-modelled dynamics and real-time implementation platform, which should be taken into account for practical application of the new controller to this process.

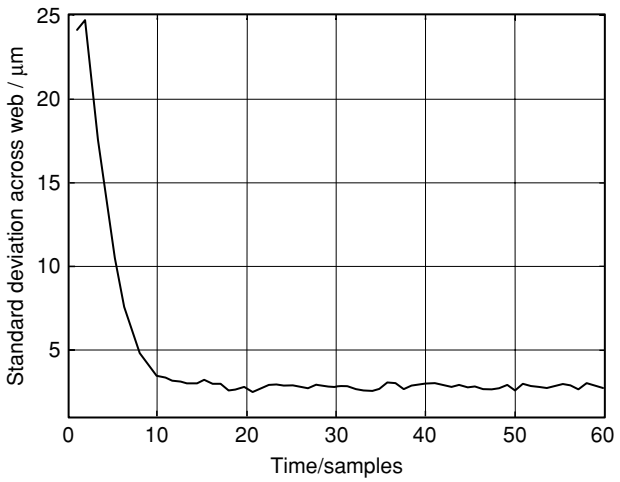

Figure 10 The transient response of the closed-loop simulation in terms of standard deviation of thickness across the web at each sample interval.

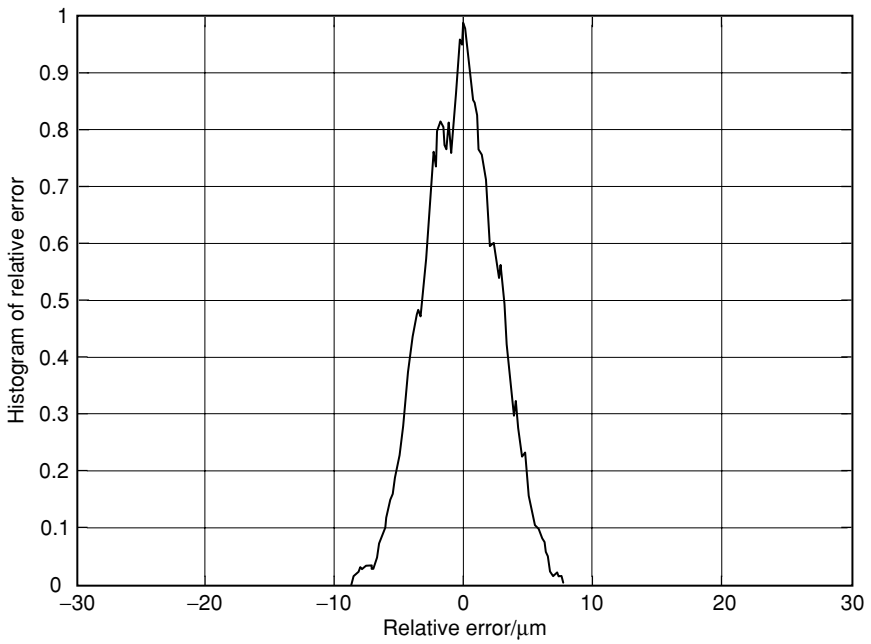

Figure 11 The steady-state response of the closed-loop simulation in terms of a histogram of thickness variations over 30 scans of the web width.

4. EXPERIMENTAL RESULTS

In Practice the principle design has been achieved through the above methodologies and simulations. Certain specific problems regarding the real-time implementation of the above scheme will be discussed next.

4.1. IMPLEMENTATION PLATFORM

The initial extrusion machine used for this study was controlled by 71 single-input single-output Proportional plus Integral (PI) controllers implemented on a 9030 series GE Fanuc Programmable Logic Controller (PLC) supported by a Programmable Co-processor Module (PCM) which runs a fast BASIC interpreter. The PCM uses a lookup table to compensate stentering effect. It implements an algorithm which compensates for web shrinkage between the die and the scanning head and gives some lateral averaging of the data. The main function of the PCM is to handle data from the infrared scanning head, which transmits thickness data as an encoded string via a serial communications link. The resulting PCM provides 71 individual thickness measurements corresponding to the 71 heated die bolts to the controller. Each PI controller output is applied to the related heater bolts as Pulse Width Modulated (PWM) signals via solid state relays.

The BASIC language interpreter in the PCM is quite suitable for implementing the complex matrix manipulations, which are required to implement the LQ control scheme. However, because of speed and memory limitations the manipulations of the large (142×142) matrices in order to calculate the control effort and at the same time capture data and manipulate the web thickness values within the available time was not possible. The GE Fanuc PLC itself incorporates 16 bit integer arithmetic including array addition and multiplication instructions. Fortunately small off-diagonal elements of model 20 or 23 decay rapidly and the number of calculations can be enormously reduced by making use of the diagonal dominance of the system equations. Even with the reduced matrices, attempting to force the complete control calculation within one scan of the PLC would effectively freeze out all other functions being performed. Yet the control loop sampling time of 38 seconds in reality gives plenty of time for the calculations to be performed. The solution to this problem is to spread the matrix calculations over several scans of the PLC. An index is used to point to a matrix row/column. Each scan, the row/column are multiplied and the index updated ready for the next scan. The matrices were scaled to use the full dynamic range available with 16-bit integer representation without risk of the overflow.

4.2. REAL-TIME IMPLEMENTATION OF THE DESIGNED CONTROL ALGORITHM

Following successful identification experiments, the control scheme was developed through the above computations presented in previous sections. The successful simulation tests of closed–loop response of the system in a simulated environment followed by the controller implementation on PLC. In industrial implementation of control algorithms in real time, testing and debugging are major problems in developing the PLC controller software. In order to overcome these problems without jeopardising plant production, PLC was connected to a PC, which effectively simulates the plant and scanning head. The closed-loop simulation results obtain in this way matched the closed-loop simulation results obtained in section 3.2. This guarantees the success of final stage, i.e. the successful mutual operation of the PLC (new controller) and plant under consideration.

It must be noted that a clear improvement in performance of implemented advanced control schemes on real processes can be difficult to demonstrate. This is because of restrictions on the process variables, difficulties of applying load disturbances and the fact that real process noise is rarely reproducible. Figure 12 shows two sets of results taken under comparable conditions as the process is started from incorrect initial conditions. The Figure 12 shows the standard deviation of thickness measured across the web at each sample interval. Further, data from the edges of the film have not been included since these are invariably out of specification due to shrinkage.

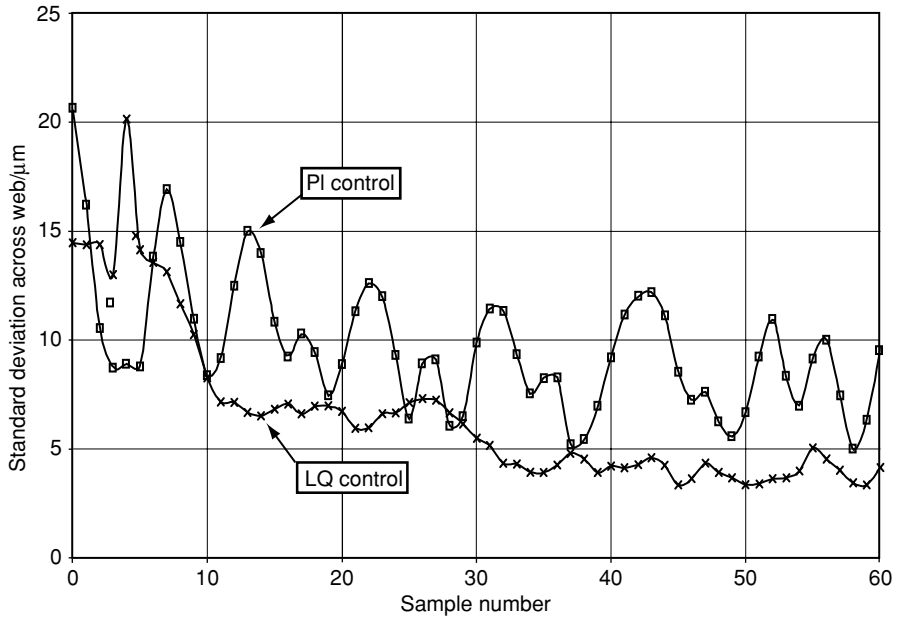

Figure 12 Start up performance of the two control schemes.

The material edges are removed later in the process for recycling. The optimal controller clearly provides tighter control than the PI controller does. In addition, the settling time is significantly faster for the optimal controller. It should be noticed that Figure 12 shows the machine start up response, i.e., when molten polymer is driven not by a steady rate. This is not the case in section 2.1 and is not true assumption in the proposed model Eqn 19 and therefore will effect the start up performance of the model-base controller. However, it is obvious from Figure 12 that although the model-free PI controller is well tuned by expert operator, still faster and better performance is obtained by model-based LQ controller.

Maintaining flow conditions, extrusion pressure, and temperature distribution as well as cooling rate and film tension within satisfactory tolerances, the steady-state performance of the two control schemes is shown in Figure 13 as a histogram of film thickness taken over the surface of the film without the edges. Data for both the PI and optimal controllers was captured from 30 scans of the film width. Accordingly, the standard deviation obtained with well-tuned PI controller was 8.8μm, which is much higher than the one obtained by optimal controller.

5. DISCUSSION, CONCLUSIONS AND FURTHER WORK

Dealing with industrial multidimensional systems or distributed parameter systems is not easy. This is not only because of underlying dynamics of such processes governs by a partial differential equation or a set of them which need simultaneous solution with some sort of moving boundary conditions that themselves have to be determined from another set of partial differential equations with their own variable boundary conditions as in the case of this study. This is because the system theory including control theory has not yet been fully developed for such processes and because amount of produced data to be processed is gigantic and yet lacks appropriate computational tools to handle the resulting large scale control problem [27]. On the other hand available computational tools are all based on some

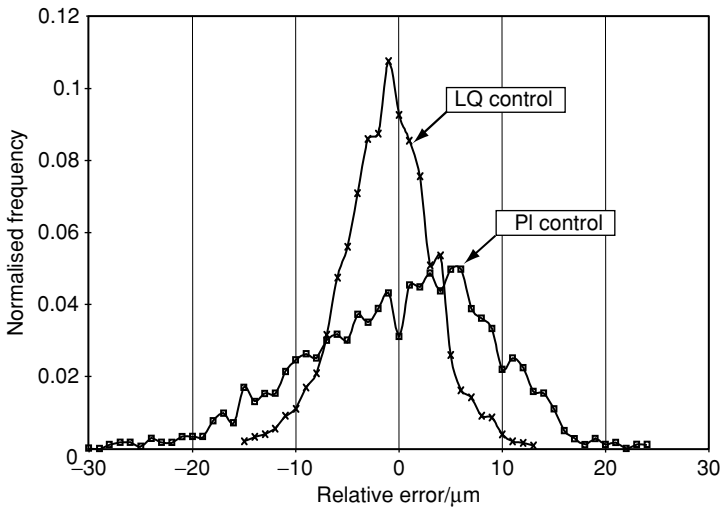

Figure 13 Histogram showing steady-state performance of the two controllers.

sort of numerical approximation, which demands further investigation on numerical accuracy and convergence [28].

Here, the Navier-Stock partial differential equations are studied analytically for a plastic extrusion process to obtain the behaviour of the fluid involved in the process. The boundary conditions for Navier-Stock equations in the process are not fixed and moving. These are determined by the solution of the thermodynamics equations governing the heat bolts die. The analytical study of the process plant has given us this insight to purpose a model structure (Eqn 19) based on the derived equations to describe the complete system from the system and control theory point of views. The purposed model structure was recognised as more suitable than the other generic 2-D models, which were studied earlier. This should be emphasised that the developed model structure should fulfil its purpose and it is not necessary for a model to stand for a thorough representation of the process under consideration. As it was discussed, there are some concerns in identifiability of 2-D discrete-continuous models for nontrivial processes. It was therefore safer choice to change the representation of model Eqn 19 to a form that is more suitable for identification and estimation purposes. Considering the fact that in 1-D systems where time is the only independent variable, there is only one way to scan the data, whereas in higher dimensions the data are often pre-digitised and processed off-line, consequently all the data are available at any time and can be proceeded in any order. It is therefore quite possible using a specific scanning regime for film thickness measurement, to make the number of outputs and number of inputs equal and represent the process plant by a square state space model (Eqn 20) based on Eqn 19. Then using the real data obtained from an identification experiment, parameters of the both models were identified. In this way concerns regarding achieving accurate parameter estimation from an unbiased estimation procedure were resolved. Further more, from practical tests it was observed that simulation of the obtained model followed real response of the process well for normal operation condition. The reasons for observed differences between process plant response and simulation in irregular operation conditions were discussed in some length. The truth is that there is no guarantee that envisaged approximated solution using even rigorous numerical methods of CFD would provide a right

answer. Even if accuracy and convergence issues of such methods are not taken into account (i.e. considering existence of a perfect numerical solution by them), because of change in rheological properties by operational condition and set point, and existence of considerable variability in the process plant day by day there is no substitute for experiments in determining rheological coefficients as well as dynamical response of the process. On the other hand one may argue that to produce a model that follow irregular operations, such extreme data should also be used in parameter estimation of the proposed models and using only open-loop step response tests are not good enough. This in turn may suggest using on-line parameter identification, nonlinear models or adaptive methods for dealing with variability in the process plant.

The Metzler form obtained for the matrix **F** in model Eqn 20 shows the obtained model present a stable process, which is true. On the other hand because of this matrix, eigenvector decomposition was considered appropriate method to solve Riccati equation (Eqn 27) for developing the optimal controller. Please note the evolution of model presentations from model Eqns 19 to 24 in order to have more accurate parameter estimation and to achieve steady-state reference tracking with no offset.

One of the common characteristics of distributed parameter systems is existence of delay differential equations in the system. Ignoring transport delay is quite dangerous as it causes instability in any closed-loop process even with the best feedback controller in the loop. The cause of transport delay in the process plant was discussed and it was taken into account for both model development and control synthesize through a predictor based on process model. However neither model nor the controller has been synthesised with the fact that time delay in the process may vary from scan to scan depending on the machine speed. Also variations of measured transport delay with the position across the film, i.e.: $d = d(i)$ were neither considered in any of the developed models nor in the control algorithm. Although one may argue that result of ZOH may compensate the effect of these variations, however it still affects the closed-loop performance. Please note that transport delay, d, was expressed as time in second in Eqn 20, i.e., $d \in R^+$, while expressed in terms of samples in Eqn 28, i.e., $d \in Z^+$.

Despite all the above difficulties, it is however shown that a significant improvement can be achieved by employment of the newly developed controller in comparison with the well-tuned model-free PI controller already in operation. The standard deviation of the web thickness variations has been reduced by more than half of the previous level and this level of performance is achieved within five to ten minutes of start-up. However, it is not unexpected that PI controller waste the first 30 minutes of the production as the process settles down. Please note model-free controllers are normally more robust than model-based controllers as variations in model representation don't affect them. Less variation in the web thickness made it possible to obtain closer result to the target thickness and facilitate significant savings in raw material.

The PLC implementation of the control scheme is far from ideal since the software is complex and difficult to maintain [29]. This reminds us of the fact which was mentioned in the beginning of this section, i.e. lack of appropriate computational hardware to handle large-scale 2-D control problems. If this limitation didn't exist, it was quite possible to perform on-line parameter estimation of an appropriate model under closed-loop feedback control, so that in each sample interval variations in the process plan would be captured and depend on operating condition and external disturbances, an automatically tuned control action would be synthesised directly or indirectly depends on control strategy [30, 31].

This exercise shows the validation of developed models for implementing complex modern control schemes and obtaining significant improvements in performance using a PLC system. The results show good promises: a significant improvement in film quality has

been achieved and notable saving in raw material and wastage are likely to result. It is of significant importance to recommend the need for serious research in areas such as stability of multidimensional systems and the effect of two directional scanning process for such complex systems.

ACKNOWLEDGEMENTS

The author gratefully acknowledge Dr Mustapha Soufian, Dr Arezki Slaouti and Mr Andy A. Verwer of the Engineering Department, Manchester Metropolitan University and also the management of Taco Plastic Ltd, especially A. S. Billings for providing the possibility to implement control algorithm on their plastic extrusion process.

REFERENCES

[1] Wang, X.G., Dumont, G.A. and Davies, M.S., "Modelling and Identification of Basis Weight Variations in Paper Machines". *IEEE Trans. on Control System Technology* , 1993, Vol. 1, No. 4, pp. 230–237.

[2] Dumont, G.A., Jonsson, I.M., Davies, M.D., Ordubadi, F.T., Fu,Y., Natarajan, K., Lindeborg, C. And Heaven, E.M., "Estimation of Moisture Variations on Paper Machines". *IEEE Trans. on Control System Technology*, 1993, Vol. 1, No. 2, pp. 101–113.

[3] Halouskova, A., Karny, M. And Nagy, I., "Adaptive Cross-direction control of Paper Basis Weight". *Automatica*, 1993, Vol. 29. pp. 425–429.

[4] Laughlin, D.L., Morari, M. And Braatz, R.D., "Robust Performance of Cross-directional Basis weight Control in Paper Machines". *Automatica*, 1993, Vol. 29. pp.1395–1410.

[5] Bergh, L.G. and Macgregor, J.F., "Spatial Control of Sheet and Film Forming Processes". *The Canadian Journal of Chemical Engineering*, 1987, Vol. 65, pp. 148–155.

[6] Boyle, T.J., "Control of Cross-Direction Variation in web Forming Machines". *The Canadian Journal of Chemical Engineering*, 1977, Vol. 55, pp. 457–461.

[7] Levy, S. and J.F. Carley, "Plastic Extrusion Technology Handbook". 2nd Edition. Industrial Press Inc. 1989.

[8] Park, W.R. and Williams, R.R., "Plastic Film Technology". Van Nostrand Reinhold, 1969.

[9] Anderson Jr, J. D. "Computational Fluid Dynamics" McGraw Hill. 1995.

[10] Versteeg, H. K. & Malalasekera, W. "An introduction to Computational Fluid Dynamics" Longman 1995.

[11] Eykhoff P. "*System Identification*." John Wiley. U.K. 1974.

[12] Soufian, M. and M. Soufian "On Data-based Modelling Techniques for Reciprocal Space of NMR imaging" *'The Third IFAC Symposium on Modelling and Control of Biomedical System'*, Warwick, U.K. 1997.

[13] Thomson, M., Schooling, S.P. and Soufian, M. "The Practical Application of a Non-linear Identification Methodology" *Control Eng. Practice*, 1996, Vol. 4. No. 3. pp. 295–306.

[14] Soufian, M., Soufian, M. and M. Thomson "Practical Comparison of Neural Networks and Conventional Identification Methodologies" on *Fifth International Conference on Artificial Neural Networks*, Cambridge, U.K. 1997.

[15] Vander Luge A. " Operational Notation for the analysis and synthesis of optical data-processing systems, Proc. IEEE Vol. 45, pp 1055–1063, 1966.

[16] Wellstead, P. E. and Zarrop, M. B. "Self-tuning Systems: Control and Signal Processing" John Wiley, 1991.

[17] Habibi A. "Two-Dimensional bayesian estimate of image" *Proc . IEEE*, 1972, Vol. 60, pp 878–883.

[18] Givone D.D. and R.D. Roesser "Multi-dimensional linear iterative circuit: General properties" *IEEE trans. On Comput*, 1972, Vol. C-21, pp 1067– 1073.

[19] Rosser R. "A Discrete state-space model for linear image processing" *IEEE Trans. AC*, 1975, Vol. AC 20, No.1.

[20] Fornasini E. & G.Marchesini. "State-Space Realisation Theory of Two-Dimensional Filters" *IEEE Trans. on AC*, 1976, Vol. AC21, No. 4.

[21] Porter W.A. and J.L. Aravena "1-D models for M-D processes" *IEEE Tran. On CKT & SYS.* , 1984, pp 742–744.

[22] Barnett, S. "Matrices Methods and Applications Clarendon Press, Oxford 1990.

[23] Soufian, M., A. Verwer, and M(u). Soufian, Model Structure and Control of a Plastic Extrusion Process, 'Multi-dimensional systems (NDS'98)' July 1998, Poland.

[24] NAG Fortran Library Manual, Mark 21, NAG Ltd, 2006.

[25] NAG C Library Manual, Mark 8, NAG Ltd, 2005.

[26] MATLAB user's guide, MathWorks Inc. 1993.

[27] Efe, M.O., Ozbay, H. Proper Orthogonal Decomposition For Reduced Order Modeling: 2D Heat Flow, IEEE Conference on Control Applications, CCA, 2003.

[28] J. Borggaard and J. Burns, Virginia Tech, Blacksburg, VA; L. Zietsman, Computational Challenges in Control of Partial Differential Equations, 2nd AIAA Flow Control Conference, Portland, Oregon, 2004.

[29] Lewis R W; "Programming industrial control systems using IEC 1131-3", IEE, London, 1995.

[30] Heath, P. Self-Tuning Control for Two-Dimensional Processes John Wiley & Sons Inc, 1994.

[31] Astrom, K.J. and Wittenmark, B. Adaptive Control 2 edition, Prentice Hall 1995.

NOMENCLATURE

c	specific heat
d	transports delay
D	Die gap
g	gravity acceleration
h	convection heat transfer coefficient,
k_t	thermal conductivity
k	pseudo-plasticity index
m	mass
n	consistency index
n_y	number of die bolts
P	pressure
P, Q	symmetric, positive semi-definite matrices
Q	flow rate
Q_{intr}, Q_{loss}	heat
S	area or cross section
S_{Mx}, S_{My}, S_{Mz}	surface or body stresses
t	time
T	sampling time
u	input
V_x, V_y, V_z	components of velocity
x, y, z	co-ordinates, distances
x	measured thickness

X	augmented state
Y	augmented output
α	expansion coefficient
$\dot{\gamma}$	shear rate
θ	temperature
ρ	density
τ_{ij} $i, j=\{x,y,z\}$	shear stress